Chapter 1

Theory of neutrino physics

Just give a short overview of the historical context, but mainly focusing on the actual description of the neutrino theory, mostly stating the fact rather than giving a large background

I should discuss everything that is even briefly mentioned in the neutrino magnetic moment theory section.

- Dirac vs Majorana neutrinos
- Neutrino masses
- Neutrino interactions with electrons and nuclei
- Neutrino oscillations and their implications

The story:

1. Brief history up to neutrinos being in the SM
2. Description of neutrinos in the SM
3. Interactions of neutrinos and their detection
4. Production of neutrinos
5. Solar and atmospheric neutrino anomalies and neutrino oscillations
6. Detail of neutrino oscillations for three flavours
7. Current state of neutrino oscillation measurements
8. Mass ordering, octant, delta CP
9. Neutrino masses - generation and measurements

Neutrinos were first introduced by Wolfgang Pauli [1, 2] as very light electrically neutral particles with half-spin and a possible magnetic moment [3]. They were a crucial part of Enrico Fermi's successful theory of β decays [4, 5], which solidified their importance in particle physics even before their first experimental detection. Fermi's theory developed into the Standard Model (SM) of particle physics [6–8], which in its current form contains three generations of fermions. Each generations contains two quarks, one charged lepton and an associated neutrino with no mass or magnetic moment.

SM is mathematically described by a Lagrangian, in which neutrinos are expressed as two-component left-handed chiral fields $\nu_{\alpha L}$, where $\alpha = e, \mu, \tau$ denotes the three neutrino generations, also called flavours [9–11]. Neutrinos form weak isospin doublets with their associated left handed charged lepton fields α_L. Unlike for the charged leptons, there is no right handed neutrino singlet in the SM. This means that neutrinos cannot obtain a (Dirac) mass term, since the mass terms for fermions arise from the Higgs mechanism [12–14] via the Yukawa coupling of the fermion and the Higgs fields [15], which requires a combination of left-handed and right-handed fields [16].

The interaction terms for neutrinos can be separated into two parts, describing the Charged current (CC) and the Neutral Current (NC) interactions, based on whether they interact with the W_μ or Z_μ massive gauge fields, which describe the $W^\pm$ or Z^0 weak boson respectively. Neglecting the non-neutrino components, the two neutrinos interaction terms are [16]

$$\mathcal{L}_{\text{CC}}^{\text{SM}} = -\frac{g_w}{2\sqrt{2}} j_W^\mu W_\mu + \text{h.c.}, \quad \text{and} \quad \mathcal{L}_{\text{NC}}^{\text{SM}} = -\frac{g_w}{2\cos(\theta_W)} j_Z^\mu Z_\mu. \tag{1.1}$$

Here g_w is the weak coupling constant, θ_W is the Weinberg angle and j_W^μ and j_Z^μ are the weak currents expressed as

$$j_W^\mu = 2 \sum_{\alpha=e,\mu,\tau} \overline{\nu}_{\alpha L} \gamma^\mu \alpha_L, \tag{1.2}$$

$$j_Z^\mu = \sum_{\alpha=e,\mu,\tau} \overline{\nu}_{\alpha L} \gamma^\mu \nu_{\alpha L}, \tag{1.3}$$

where γ^μ, $\mu = 0, 1, 2, 3$, are the four Dirac gamma matrices.

The two terms of the interaction Lagrangian from Eq. 1.1 describe the possible neutrino interaction vertices shown in Fig. 1.1. These diagrams show the CC and the NC interaction of neutrinos and antineutrinos and, in case of the CC diagram, can also be flipped around the vertical axis to show the production of neutrinos from the weak interaction (or decays) of leptons. They can also be rotated $90°$ to either show the annihilation, or the production of the neutrino-lepton (for CC), or neutrino-antineutrino (for NC) pairs.

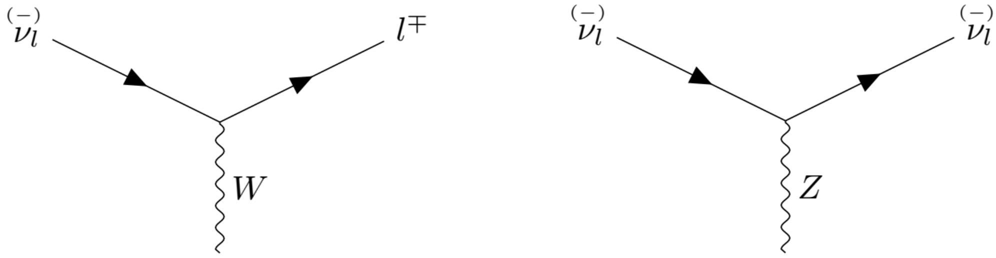

Figure 1.1: Neutrino interaction vertices in the SM via the weak charged currents (left) and the neutral currents (right).

1.1 Neutrino Production

Some of the most common neutrino and antineutrino production channels include nucleon transitions via CC weak interactions. Specifically, the transition of a neutron into a proton, either as a decay of a free neutron, or as a β^- decay for neutrons bound in a nucleus, produces an electron and an electron antineutrino:

$$n \to p + e^- + \overline{\nu}_e. \tag{1.4}$$

The study of the shape of the electron spectrum from β^- decay was the reason Pauli proposed the existence of the neutrino [1]. Additionally, this channel is an abundant source of $\overline{\nu}_e$ from nuclear reactors, which were the first artificial sources of neutrinos, increasing the neutrino flux by about 100 million compared to the naturally occurring sources, enabling the first ever detection of a neutrino [17–19].

Similarly, the production of an electron neutrino via the transition of a proton into a neutron can occur inside the nucleus either as the β^+ decay:

$$p \rightarrow n + e^+ + \nu_e, \tag{1.5}$$

or via the electron capture:

$$p + e^- \rightarrow n + \nu_e. \tag{1.6}$$

This channel occurs in stars and in the first phase of supernovae [16].

However, most supernovae neutrinos are created via a thermal pair production via NC interaction

$$e^- + e^+ \rightarrow \nu_\alpha + \overline{\nu}_\alpha \tag{1.7}$$

producing neutrinos and antineutrinos of all flavours. Neutrino pair production via the decay of Z^0 was studied in great detail [20], since the magnitude of the decay width depends on the number of light active neutrino flavours, with the current best fit $N_\nu = 2.984$ [21].

An abundant source of ν_μ and $\overline{\nu}_\mu$ is the decay of pions and muons

$$p + X \rightarrow \pi^\pm \rightarrow \mu^\pm + \nu_\mu \left(\overline{\nu}_\mu\right) \tag{1.8}$$

$$\mu^\pm \rightarrow e^\pm + \nu_\mu \left(\overline{\nu}_\mu\right) + \nu_e \left(\overline{\nu}_e\right), \tag{1.9}$$

which naturally occurs in Earth's atmosphere from the interaction of cosmic ray protons. It is notable, that if all the muons decay by the time they reach Earth's surface, the ratio of $\nu_\mu : \nu_e$ should be exactly 2:1. This processed is also used in the modern accelerator-based sources of neutrinos, which accelerate protons to the desired energies, impinge them onto a fixed target, and focus the resulting hadrons to achieve a highly pure and precise source of ν_μ or $\overline{\nu}_\mu$ [22, 23]. Similarly, decays of heavier hadrons, such as kaons and charmed particles, also produce neutrinos, including ν_τ and $\overline{\nu}_\tau$ [24, 25].

1.2 Neutrino Interactions

The interaction of neutrinos can either be categorized based on the target, which is generally either electron or a nucleus, or on the neutrino energy.

Neutrino-electron interactions occur either via elastic scattering, which result in a neutrino and an electron in the final state, or via the inverse muon (or tau) decay, which contains a muon (or tau) in the final state. Both of these interactions are purely governed by Quantum Electro Dynamics (QED) and are theoretically very well understood, and we are currently using their measurements to provide constraints on the parameters within the QED theory. Additionally, while the neutrino-on-electron elastic scattering does not have a threshold energy and can occur for any neutrinos, the inverse muon decay has a threshold for the ν_μ energy of $10.92\,\mathrm{GeV}$, and the inverse tau decay $E_{\nu_\tau} > 3\,\mathrm{TeV}$ [16, 26].

The interaction of neutrinos with a nucleus can be to an extent approximated by an interaction of neutrinos on quasi-free nucleons [27]. The interaction of neutrinos on nucleons can be further classified based on the products it generates. We illustrate these categories on a case of ν_μ CC cross section in Fig. 1.2. At lower energies neutrinos interact via the elastic interactions in the NC channel, simply kicking the nucleon out of the nucleus, and via the Quasi Elastic (QE) interactions in the CC channel, transforming the neutron or proton into its nucleon counterpart. For example, the QE interaction of an antineutrino on a proton

$$\overline{\nu}_l + p \to n + l^+ \tag{1.10}$$

is often called the inverse β decay and it was used for the first ever detection of neutrinos (specifically electron antineutrinos from a nuclear reactor) by Cowan and Reines [17, 18]. Analogically, the interaction of neutrinos on a neutron

$$\nu_l + n \to p + l^- \tag{1.11}$$

is interesting especially due to having no low energy threshold for ν_e and it is commonly used for detection of solar neutrinos [28]. For ν_μ and ν_τ there is a low energy threshold for the QE interactions on a free nucleon. For ν_μ this threshold is about $110\,\mathrm{GeV}$, which can be clearly seen in Fig. 1.2 as the drop off cross section at low energies. The ν_μ CCQE channel was used for the first detection of ν_μ [29] from an accelerator and is commonly used for the detection of atmospheric neutrinos [30–32]. The threshold for the CCQE interaction of ν_τ is about $3.5\,\mathrm{GEV}$, which meant that it was only discovered only in 2000 by the DONUT Collaboration at Fermilab [24].

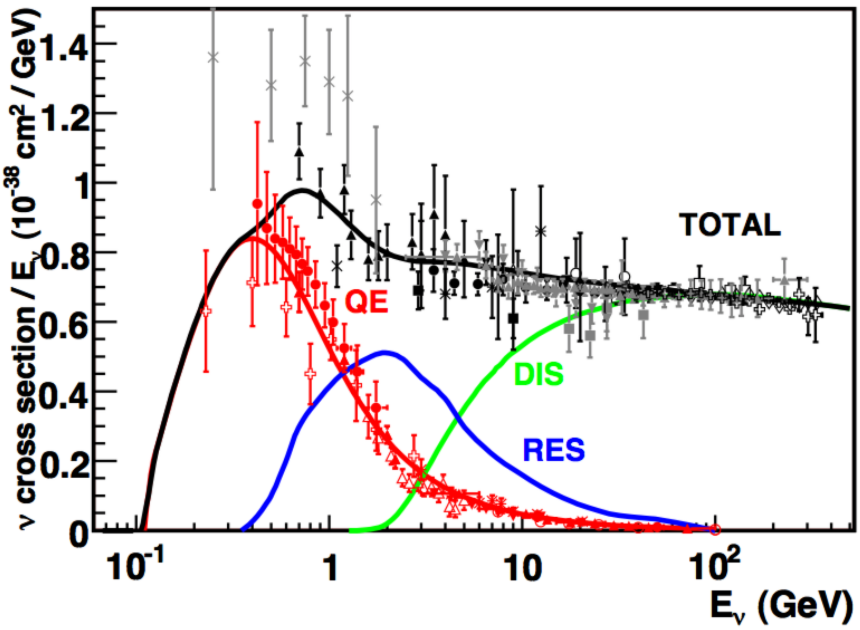

Figure 1.2: Neutrino CC cross sections on an isolated nucleon divided by the neutrino energy based on the interaction types. Figure is from [33] and compares the measured data [27] and the prediction provided by the NUANCE generator [34].

With an increase in neutrino energy above a certain threshold (about $270\,\mathrm{MeV}$ for ν_μ), neutrinos start the Resonant baryon production (RES), which commonly decay into a nucleon and an additional hadron. These hadrons are initially pions at lower energies, but by increasing the neutrino incident energy, they start producing multiple pions and other mesons and hyperons. With even higher incident energies, neutrinos start probing the quark contents of the individual nucleons in the Deep Inelastic Scattering (DIS) interaction, as can be seen in Fig. 1.2.

Even though the approximation of nuclei as collections of quasi-free nucleons is useful, it has been shown [35] that there are important nuclear effects that have to be considered. Example of these are: Fermi motion of nucleons and their binding inside the nucleus, Pauli's exclusion principle and nucleon energy levels, short and long range nucleon-nucleon correlations, Meson Exchange Current (MEC), or Final State Interaction (FSI) [36].

Additionally, if the total energy transferred to the nucleus is small relative to the size of the nucleus, neutrinos can interact with the entire nucleus coherently. At low energies, neutrinos can interact via the Coherent Elastic ν Nucleus Scattering (CEvNS), where the contributions from each individual nucleon are simply added together coherently [37], leaving behind an excited nucleus. At higher energies, neutrinos can interact via the Coherent pion production (COHπ) without transferring much momentum to the nucleus. Therefore, there is only a single pion produced (charged through CCCOHπ and neutral through NCCOHπ), which receives most of the transferred momentum and generally travels in the direction of the initial neutrino. This means that the COHπ can mimic real $\mu^{\pm}$, e^{-}, or γ signal in a detector [36].

Another notable example is the two particle - two hole (2P2H) interaction [38–40], which occurs when neutrinos interact with a correlated pair of nucleons, resulting in two nucleons leaving the nucleus, which now has two holes. This interaction can significantly increase the QE cross section [36]. Most frequently, this interaction occurs via the MEC, where the meson effectively propagates the interaction between the two bound nucleons.

The products of each of the aforementioned interactions can re-interact inside the nucleus in the so-called FSI. The final products of the interaction will therefore make it appear as a different interaction inside the detector.

1.3 Neutrino Oscillation

The idea that neutrinos can oscillate originates [41, 42] from the already known oscillations of $K^0 \leftrightarrow \overline{K^0}$. This was adapted to the oscillations between different neutrino flavours [43, 44] by considering that the weak interaction neutrino eigenstates ν_α, produced in CC weak interactions described in Eq. 1.1-1.3, are not identical to the mass neutrino states ν_k, which are the eigenstates of the hamiltonian[1]

$$\mathcal{H} \left|\nu_k\right\rangle = E_k \left|\nu_k\right\rangle . \tag{1.12}$$

From the Schrödinger equation

$$i\frac{d}{dt} \left|\nu_k\left(t\right)\right\rangle = \mathcal{H} \left|\nu_k\left(t\right)\right\rangle \tag{1.13}$$

[1]vacuum hamiltonian, for the full hamiltonian including interactions with matter see matter effect below

we get that the massive neutrino states evolve as plane waves

$$|\nu_k(t)\rangle = e^{-iE_k t}|\nu_k\rangle . \tag{1.14}$$

The energy of the neutrino state

$$E_k = \sqrt{\vec{p}^{\,2} + m_k^2} \tag{1.15}$$

can be approximated as

$$E_k \xrightarrow{m^2 \ll p^2 \approx E^2} E + \frac{m_k^2}{2E}, \tag{1.16}$$

for ultra-relativistic neutrinos [16]. Additionally, given the notation $c \equiv 1$, we can approximate $L \approx t$, where L is the distance neutrino travelled in time t, also called the baseline, which is easier to be experimentally measured than time.

The neutrino flavour and mass eigenstates are related by

$$|\nu_\alpha\rangle = \sum_k U_{\alpha k}^* |\nu_k\rangle , \tag{1.17}$$

where U is a unitary matrix now known by the authors of neutrino oscillations as the Pontecorvo-Maki-Nakagawa-Sakata (PMNS) matrix [16, 45]. Due to its unitarity, the inverse relation is simply

$$|\nu_k\rangle = \sum_\alpha U_{\alpha k} |\nu_\alpha\rangle . \tag{1.18}$$

Given that $\langle \nu_k | \nu_j \rangle = \delta_{kj}$ and $\langle \nu_\alpha | \nu_\beta \rangle = \delta_{\alpha\beta}$ and using Eq. 1.14,1.17 and 1.18, we can write the amplitude of the $\nu_\alpha \to \nu_\beta$ transition over the distance L as

$$A_{\nu_\alpha \to \nu_\beta}(L) \equiv \langle \nu_\beta | \nu_\alpha(L) \rangle = \sum_k U_{\alpha k}^* U_{\beta k} e^{-iE_k L} \tag{1.19}$$

and the probability as

$$P_{\nu_\alpha \to \nu_\beta}(L) = \left| A_{\nu_\alpha \to \nu_\beta}(L) \right|^2 = \sum_{k,j} U_{\alpha k}^* U_{\beta k} U_{\alpha j} U_{\beta j}^* e^{-i(E_k - E_j)L}. \tag{1.20}$$

Given Eq. 1.16 and defining the neutrino mass splitting as

$$\Delta m_{kj}^2 \equiv m_k^2 - m_j^2, \tag{1.21}$$

we get

$$P_{\nu_\alpha \to \nu_\beta}(L) = \sum_{k,j} U^*_{\alpha k} U_{\beta j} U_{\alpha j} U^*_{\beta j} e^{-i\frac{\Delta m^2_{kj} L}{2E}}. \tag{1.22}$$

There can be in general any number of neutrino mass and flavour eigenstates. However, given we know three neutrinos flavour states, ν_α, where $\alpha = e, \mu, \tau$, we consider a symmetric 3×3 PMNS matrix parametrized as:

$$U = \begin{pmatrix} U_{e1} & U_{e2} & U_{e3} \\ U_{\mu 1} & U_{\mu 2} & U_{\mu 3} \\ U_{\tau 1} & U_{\tau 2} & U_{\tau 3} \end{pmatrix} =$$

$$= \begin{pmatrix} 1 & 0 & 0 \\ 0 & c_{23} & s_{23} \\ 0 & -s_{23} & c_{23} \end{pmatrix} \begin{pmatrix} c_{13} & 0 & s_{13}e^{-i\delta} \\ 0 & 1 & 0 \\ -s_{13}e^{i\delta} & 0 & c_{13} \end{pmatrix} \begin{pmatrix} c_{12} & s_{12} & 0 \\ -s_{12} & c_{12} & 0 \\ 0 & 0 & 1 \end{pmatrix}, \tag{1.23}$$

where $c_{ij} \equiv \cos\theta_{ij}$ and $s_{ij} \equiv \sin\theta_{ij}$. The matrix is parametrized using three mixing angles θ_{12}, θ_{13} ,and θ_{23}, which in general define the amplitude of neutrino oscillation. Additionally, there is one phase often denoted as the δ_{CP} phase, which describes the possible Charge conjugation - Parity (CP) violation for neutrino oscillations. Specifically, if the value of the δ_{CP} is different from $N\pi$, where $N \in \mathbb{Z}$, it would imply the CP symmetry violation and therefore a difference between neutrino and antineutrino oscillations.

From Eq. 1.22, we can see that the frequency of neutrino oscillations depends on the Δm^2. In case of three neutrino mass states, there are two independent mass squared differences. Other than the PMNS matrix, neutrino oscillations depend on the mass squared differences (eq.1.21). In case of 3 neutrinos, those are Δm^2_{21} and Δm^2_{31}. Δm^2_{21} mainly drives oscillations of solar neutrinos and is therefore often denoted as $\Delta m^2_{\odot}$ or Δm^2_{sol}, while Δm^2_{31} drives oscillations on the scale for atmospheric neutrinos and is often written as Δm^2_{atm} [45]. TO DO: *Update this and mention that this means that there must be at most one massless neutrino states and neutrinos must have mass*

The idea of neutrino oscillations was suggested as an explanation for the observed deficit of solar neutrinos [28] and for the disagreement between the measurement and the prediction for the $\nu_\mu : \nu_e$ fraction of the atmospheric neutrinos [46–49]. The so-called atmospheric neutrino anomaly was resolved by the Super-Kamiokande

(SK) experiment [50], which reported the first evidence for neutrino oscillations. The solar neutrino anomaly was resolved by the Sudbury Neutrino Observatory (SNO) experiment [51], which compared the rate of the CC interaction, which are affected by neutrino oscillations, and of the NC interaction, which can't determine between neutrino flavours and are therefore unaffected by neutrino oscillations. However, the results from SNO confirmed that we need to account for so-called matter effects, especially for solar neutrinos.

1.3.1 The Matter Effect

The hamiltonian in Eq. 1.12 and all the previous considerations only consider neutrino oscillations in vacuum, without possible interactions in matter. To account for the effect of matter on neutrinos oscillations, also called the Mikheyev-Smirnov-Wolfenstein (MSW) effect [52, 53] after its discoverers, we can consider $\mathcal{H} = \mathcal{H}_0 + \mathcal{H}_I$, where

$$\mathcal{H}_I \left|\nu_\alpha\right\rangle = V_\alpha \left|\nu_\alpha\right\rangle . \tag{1.24}$$

This potential V_α will be different for electron neutrinos and for the other flavours, as ν_e can have CC interaction with electrons, which are abundant in the universe unlike the other charged leptons [16]:

$$V_\alpha = V_{\text{CC}}\delta_{\alpha e} + V_{\text{NC}} = \pm\sqrt{2}G_F \left(N_e \delta_{\alpha e} - \frac{1}{2} N_n \right) , \tag{1.25}$$

where G_F is the Fermi coupling constant, N_e is the electron density, N_n is the neutron density and the plus and minus signs is for neutrinos or antineutrinos respectively.

This potential effectively shifts the values of the mixing angles and the mass squared differences based on the matter neutrinos pass through and shifts it in the opposite direction for neutrinos and antineutrinos.

Should probably also mention that this is of particular interest to the solar neutrinos...

Currently the three neutrino paradigm is well established. The absolute values (magnitudes) of the two neutrino mass splitting are well measured, two of the mixing angles are known fairly well θ_{13} and θ_{12} and for the third θ_{23} we know it is close to the maximum, but still trying to figure out whether it is $< 45°$ or $> 45°$, also called the octants. We still don't know what is the δ_{CP} [54].

Global fit [55]

δ_{CP} could help explain the matter antimatter asymmetry in the universe The fact that the Universe consists of matter and not antimatter hints at a fundamental asymmetry between matter and antimatter, in the form of CP violation. We know that the known sources of CP violation via quark mixing and from the QCD Lagrangian are insufficient to account for the composition of the Universe. Neutrino oscillation is sensitive to one new CP phase and if neutrinos are Majorana particles, there are two additional neutrino-sector CP phases which may contribute to matter-antimatter asymmetry [54].

Need to mention the importance of the δ_{CP} measurements, maybe even the Sakharov conditions... Also why do we care about the Δm^2 or the octants and what are those... Maybe cite the Snowmass report and the PDG.

[IUPAP˙Neutrino˙Panel˙Report˙2021.pdf] Neutrinos oscillate which implies that leptons mix in analogy to quarks. This means that neutrinos have non-vanishing rest masses, which requires at least one new particle species beyond the ones in the standard model.

[IUPAP˙Neutrino˙Panel˙Report˙2021.pdf] The size of the matter effect depends on the density and composition of the medium and on the oscillation parameters. In particular, the matter effect may be exploited to determine the octant of the mixing angles and the sign of the mass-squared differences. Moreover, the matter effect is different for neutrinos and antineutrinos because for the latter A changes sign. The difference between the oscillation probabilities of neutrinos and antineutrinos that arises from the matter effect must be taken into account in searches for CP-invariance violation. The CP-invariance violation arising from δ_{CP} must be distinguished from that which arises due to the matter effect. This can be accomplished by exploiting the differences in the modulations of the four oscillation probabilities ν_e appearance, $\overline{\nu}_e$ appearance, ν_μ disappearances and $\overline{\nu}_\mu$ disappearance.

[56] These observations, subsequently confirmed using neutrinos produced in nuclear reactors and at accelerator facilities, established that the three-flavor oscillations of Eq. (4) can be described to a good approximation by two, decoupled oscillations. The first, describing the oscillations of atmospheric muon neutrinos, is characterized

by a large mass-squared difference and a mixing angle that is approximately 45 degrees. The second, describing the oscillations of solar electron neutrinos, is characterized by a small mass-squared splitting and a large (approx. 35 degrees) mixing angle. θ_{23} is referred to as the "atmospheric mixing angle" as it determines at leading order the oscillations of atmospheric muon neutrinos while θ_{12} is referred to as the solar mixing angle as it is used, at leading order, to describe the oscillations of solar electron neutrinos. The mixing angle θ_{13} is small, accounting for the approximate decoupling of the atmospheric and solar oscillations. For Majorana neutrinos there are two additional phases ("Majorana phases"), which an be put in a diagonal phase matrix to the right of Eq.(5). See Sec. 5.3 for a discussion. Two additional phases that might arise if neutrinos are Majorana particles can not be measured in neutrino-oscillation experiments and are omitted from Eq. (5).

1.4 Neutrino Mass

The existence of non-zero neutrino mass is, to date, the only laboratory-based observation of BSM physics. The disparity of mass scales between neutrinos and other fundamental particles suggests a high-energy scale for neutrino-mass generation. In models where this mechanism lies at or below the TeV scale, the physics of neutrino mass may be accompanied by complementary signatures at colliders. In models where the scale is higher, experiments probing the nature of neutrino mass are the only feasible way of exploring this new physics. The observation of neutrinoless double beta decay would provide direct evidence that lepton number is violated, opening a path to baryogenesis via leptogenesis in the early universe. As such, direct tests of the scale or nature of neutrino mass target some of the most central open questions in fundamental physics today. Other neutrino properties may be connected to extensions of the standard model, yet are not observable via oscillations. Neutrino electromagnetic properties are of fundamental interest, [54].

Detection of neutrinoless double beta decay is the only known method with plausible sensitivity to the Majorana nature of the neutrino, one of the most important open questions in particle physics. [54]

Experiments for their values? Theoretical predictions for how they obtained them

Theories of neutrino mass generation

[Fundamentals of neutrinos physics and astrophysics] The only extension of the SM that is needed is the introduction of right-handed components $\nu_{\alpha R}$ of the neutrino fields. Such a model is sometimes called the *minimally extended Standard Model.* The right handed neutrino fields are fundamentally different from the other elementary fermion fields because they are invariant under the symmetries of the SM: they are **singlets** of $\mathrm{SU}(3)_C \times \mathrm{SU}(2)_L$ and have hypercharge $Y = 0$. The right handed neutrino fields are called sterile [883] because they do not participate in weak interactions and their only interaction is gravitational. their right handedness is not required though! could also be left handed but have to be singlets and therefore sterile!

In the minimally extended standard model with three right handed neutrino fields, the SM Higgs-lepton Yukawa Lagrangian is extended by adding a lepton term with the same structure as the second term on the right handed side, which generates the masses of up-type quarks

$$\mathcal{L}_Y = -\sum_{\alpha,\beta=e,\mu,\tau} Y'^{l}_{\alpha\beta}\overline{L}_{\alpha L}\Phi l'_{\beta R} - \sum_{\alpha,\beta=e,\mu,\tau} Y'^{\nu}_{\alpha\beta}\overline{L}_{\alpha L}\tilde{\Phi}\nu'_{\beta R} + \text{h.c.}, \tag{1.26}$$

where Y'^{ν} is a new matrix of Yukawa couplings.

Using the unitary gauge we can diagonalize the Yukawa couplings we obtain

$$\mathcal{L}_Y = -\sum_{\alpha=e,\mu,\tau} \frac{y^l_\alpha v}{\sqrt{2}}\bar{l}_\alpha l_\alpha - \sum_{k=1}^{N} \frac{y^\nu_k v}{\sqrt{2}}\overline{\nu}_k \nu_k - \sum_{\alpha=e,\mu,\tau} \frac{y^l_\alpha}{\sqrt{2}}\bar{l}_\alpha l_\alpha H - \sum_{k=1}^{N} \frac{y^\nu_k}{\sqrt{2}}\overline{\nu}_k \nu_k H \tag{1.27}$$

Therefore the neutrino masses are given by

$$m_k = \frac{y^\nu_k v}{\sqrt{2}} \quad (k = 1, ..., N)\,, \tag{1.28}$$

and massive Dirac neutrinos couple to the Higgs field through the last term. Note that the neutrinos masses are proportional to the Higgs VEV v, as the masses of charged leptons and quarks. However, it is known that the masses of neutrinos are much smaller than those of charged leptons and quarks, but there is no explanations here of the very small values of the eigenvalues Y^ν_k of the Higgs-neutrino Yukawa coupling matrix that are needed. The lagrangian defined this way does not conserve the lepton flavour number, which leads to neutrino oscillations. The Dirac character of massive neutrinos is closely related to the invariance of the total Lagrangian under the global U(1) gauge transformations.

The sterile neutrino fields do not participate in weak interaction with both their left and right components, but can couple with the ordinary neutrinos through the mass therm, generating a complicated mixing between active and sterile degrees of freedom.Since at present there is no indication of the existence of such additional sterile Dirac neutrino fields, ockham's razor suggests to ignore them...

1.4.1 Majorana neutrinos

[Fundamentals of neutrinos physics and astrophysics,p.190] If the neutrino is massless, since the left handed chiral component of the neutrino field obeys the Weyl equation in both the Dirac and Majorana descriptions and the right handed chiral component is irrelevant for neutrino interactions, the Dirac and Majorana theories are physically equivalent. From this it is clear that in practice one can distinguish a Dirac from a Majorana neutrino only by measuring some effect due to the neutrino mass. Moreover, the mass effect must not be of kinematical nature, because the kinematical effects of Dirac and Majorana masses are the same. For example, the Dirac and Majorana nature of neutrinos cannot be revealed through neutrino oscillations! The most promising way to find if neutrinos are Majorana particles is the search for neutrinoless double beta decay.

[OverviewOfNeutrinoPhysicsPheno2024.pdf] In contrast, the Majorana phases do not enter the flavour neutrino oscillation probabilities [22, 85], but contribute to the $\beta\beta_{0\nu}$ decay rate

Chapter 2

Muon Neutrino Magnetic Moment Measurement

In the standard model, neutrinos have small charge radii induced by radiative corrections. The predicted values of the electron and muon neutrino charge radii are less than an order of magnitude smaller than the current experimental upper limits and can be tested in the next generation of accelerator and reactor experiments through the observation of neutrino-electron elastic scattering and CEvNS. Precision measurements of the neutrino charge radii would either be an important confirmation of the standard model, or would discover new physics. The same types of experimental measurements are also sensitive to more exotic neutrino electromagnetic properties: magnetic moments and millicharges, which would be certainly due to new BSM physics. The discovery of millicharges or anomalously large neutrino magnetic moments would have also important implications for astrophysics and cosmology.[54]

2.1 Theory of neutrino magnetic moment

TO DO: *Re-read the three main theory papers and double check the theoretical overview*

In the Standard Model (SM), neutrinos are massless and electrically neutral particles. However, even in the SM neutrinos can have electromagnetic interaction through loop diagrams involving the charged leptons and the W boson. These interactions are described by the neutrino charge radius, described in section 2.1.2 [?].

To include neutrino masses required by neutrino oscillations, we must go Beyond the Standard Model (BSM), where neutrinos can acquire other electromagnetic properties [?]. In the most general case, considering interactions with a single photon as shown on Fig. 2.1, neutrino electromagnetic interactions can be described by an *effective* interaction Hamiltonian [?]

$$\mathcal{H}_{em}^{(\nu)}(x) = \sum_{k,j=1}^{N} \overline{\nu}_k(x)\,\Lambda_\mu^{kj}\nu_j(x)\,A^\mu(x)\,. \tag{2.1}$$

Here $\nu_k(x)\,, k \in \{1, ..., N\}$ are neutrino fields in the mass basis with N neutrino mass states. Λ_μ^{kj} is a general vertex function and $A^\mu(x)$ is the electromagnetic field.

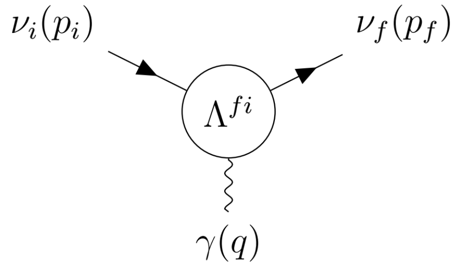

Figure 2.1: Effective coupling of neutrinos with one photon electromagnetic field 2.

The vertex function $\Lambda_\mu^{fi}(q)$ is generally a matrix and in the most general case can be written in terms of linearly independent products of Dirac matrices (γ) and only depends on the square of the four momentum of the photon $(q = p_f - p_i)$:

$$\begin{aligned}\Lambda_\mu^{fi}(q) =& \mathbb{F}_1^{fi}\left(q^2\right) q_\mu + \mathbb{F}_2^{fi}\left(q^2\right) q_\mu\gamma_5 + \mathbb{F}_3^{fi}\left(q^2\right)\gamma_\mu + \mathbb{F}_4^{fi}\left(q^2\right)\gamma_\mu\gamma_5 + \\ & \mathbb{F}_5^{fi}\left(q^2\right)\sigma_{\mu\nu}q^\nu + \mathbb{F}_6^{fi}\left(q^2\right)\epsilon_{\mu\nu\rho\gamma}q^\nu\sigma^{\rho\gamma},\end{aligned} \tag{2.2}$$

where $\mathbb{F}_i^{fi}(q^2)$ are six Lorentz invariant form factors [?].

Applying conditions of hermiticity $\left(\mathcal{H}_{em}^{(\nu)\dagger} = \mathcal{H}_{em}^{(\nu)}\right)$ and of the gauge invariance of the electromagnetic field, we can rewrite the vertex function as

$$\Lambda_\mu^{fi}(q) = \left(\gamma_\mu - q_\mu \not{q}/q^2\right)\left[\mathbb{F}_Q^{fi}\left(q^2\right) + \mathbb{F}_A^{fi}\left(q^2\right)q^2\gamma_5\right] - i\sigma_{\mu\nu}q^\nu\left[\mathbb{F}_M^{fi}\left(q^2\right) + i\mathbb{F}_E^{fi}\left(q^2\right)\gamma_5\right], \tag{2.3}$$

where $\mathbb{F}_Q^{fi}, \mathbb{F}_M^{fi}, \mathbb{F}_E^{fi}$ and $\mathbb{F}_A^{fi}$ are hermitian matrices representing the charge, dipole magnetic, dipole electric and anapole neutrino form factors. In coupling with a real photon $(q^2 = 0)$ these become the neutrino charge and magnetic, electric and anapole moments. The neutrino charge radius corresponds to the second term in the expansion of the charge form factor [?].

We can simplify the above expression as [?]

$$\Lambda_{\mu}^{fi}(q) = \gamma_{\mu}\left(Q_{\nu_{fi}} + \frac{q^2}{6}\langle r^2\rangle_{\nu_{fi}}\right) - i\sigma_{\mu\nu}q^{\nu}\mu_{\nu_{fi}}, \tag{2.4}$$

where $Q_{\nu_{fi}}$, $\langle r^2\rangle_{\nu_{fi}}$, and $\mu_{\nu_{fi}}$ are the neutrino charge, effective charge radius (also containing anapole moment), and an effective magnetic moment (also containing electric moment) respectively. This is possible thanks to the proportional effect of the neutrino charge radius and the anapole moment, or the neutrino magnetic and electric moment respectively [?]. These quantities (charge, charge radius and magnetic moment) are the three neutrino electromagnetic properties measured in experiments.

2.1.1 Neutrino electric and magnetic dipole moments

The size and effect of the neutrino electromagnetic properties depends on the specific theory beyond the standard model.

Evaluating the one loop diagrams in the minimal extension of the standard model with three right handed Dirac neutrinos gives us the first approximation of the electric and magnetic moments:

$$\left.\begin{matrix}\mu_{kj}^{D} \\ i\epsilon_{kj}^{D}\end{matrix}\right\} \simeq \frac{3eG_F}{16\sqrt{2}\pi^2}(m_k \pm m_j)\left(\delta_{kj} - \frac{1}{2}\sum_{l=e,\mu,\tau} U_{lk}^{\star}U_{lj}\frac{m_l^2}{m_W^2}\right), \tag{2.5}$$

where m_k, m_j are the neutrino masses and m_l are the masses of charged leptons which appear in the loop diagrams [?]. e is the electron charge, G_F is the Fermi coupling constant, and U is the PMNS neutrino oscillation matrix. Higher order electromagnetic corrections were neglected, but those can also have a significant contribution, depending on the theory.

It can be seen that there dirac neutrinos have no diagonal electric moments $\left(\epsilon_{kk}^{D} = 0\right)$ and their diagonal magnetic moments are approximately

$$\mu_{kk}^{D} \simeq \frac{3eG_F m_k}{8\sqrt{2}\pi^2} \simeq 3.2 \times 10^{-19}\left(\frac{m_k}{\text{eV}}\right)\mu_B, \tag{2.6}$$

where μ_B is the Bohr magneton [?].

The transition magnetic moments are suppressed with respect to the largest of the diagonal magnetic moments by at least a factor of 10^{-4} due to the m_W^2 in the denominator. The transition electric moments are even smaller due to the mass difference in Eq.2.5. Therefore an experimental observation of a magnetic moment larger than in Eq.2.6 would indicate physics beyond the minimally extended standard model [? ?].

Majorana neutrinos in a minimal extension can be obtained by either adding a $\mathrm{SU}\,(2)_L$ Higgs triplet, or right handed neutrinos together with a $\mathrm{SU}\,(2)_L$ Higgs singlet [?]. If we neglect the Feynman diagrams which depend on the model of the scalar sector, the magnetic and electric dipole moments are

$$\mu_{kj}^M \simeq -\frac{3ieG_F}{16\sqrt{2}\pi^2}\left(m_k + m_j\right)\sum_{l=e,\mu,\tau}\mathrm{Im}\left[U_{lk}^\star U_{lj}\right]\frac{m_l^2}{m_W^2}, \tag{2.7}$$

$$\epsilon_{kj}^M \simeq \frac{3ieG_F}{16\sqrt{2}\pi^2}\left(m_k - m_j\right)\sum_{l=e,\mu,\tau}\mathrm{Re}\left[U_{lk}^\star U_{lj}\right]\frac{m_l^2}{m_W^2}. \tag{2.8}$$

These are difficult to compare to the Dirac case, due to possible presence of Majorana phases in the PMNS matrices, but it is clear that they have the same order of magnitude as Dirac transition dipole moments. However, the neglected model dependent contributions can enhance the transition dipole moments [?].

It is possible [?] to obtain a "natural" upper limits on the size of neutrino magnetic moment by calculating its contribution to the neutrino mass by standard model radiative corrections. For Dirac neutrinos, the radiative correction induced by neutrino magnetic moment, generated at an energy scale Λ, to the neutrino mass is generically

$$m_\nu^D \sim \frac{\mu_\nu^D}{3\times 10^{-15}\mu_B}\left[\Lambda\left(\mathrm{TeV}\right)\right]^2 \mathrm{eV}. \tag{2.9}$$

So for $\Lambda \simeq 1$TeV TO DO: *figure out what exactly does this energy scale actually relate to and explain it here?* and $m_\nu \lesssim 0.3$eV the limit becomes $\mu_\nu^D \lesssim 10^{-15}\mu_B$. This applies only if the new physics is well above the electroweak scale ($\Lambda_{EW} \sim 100$GeV). It is possible to get Dirac neutrino magnetic moment higher than this limit, for example in frameworks of minimal super-symmetric standard model, by adding more Higgs doublets, or by considering large extra dimensions [?].

A similar limit for Majorana neutrino magnetic moment would be less stringent due to the antisymmetry of the Majorana neutrino magnetic moment form factors.

Considering $m_\nu \lesssim 0.3$eV, the limit can be expressed as

$$\mu_{\tau\mu}, \mu_{\tau e} \lesssim 10^{-9} \left[\Lambda \left(\mathrm{TeV}\right)\right]^{-2} \tag{2.10}$$

$$\mu_{\mu e} \lesssim 3 \times 10^{-7} \left[\Lambda \left(\mathrm{TeV}\right)\right]^{-2} \tag{2.11}$$

which is shown in the flavour basis [?]. This expression relates to the framework used previously as

$$\mu_{ij} = \sum_{\alpha\beta} \mu_{\alpha\beta} U^{\star}_{\alpha i} U_{\beta j}, \quad \alpha, \beta \in \{e, \mu, \tau\}\,. \tag{2.12}$$

These considerations imply, that if a magnetic moment $\mu \gtrsim 10^{-15}\mu_B$ would be measured, it is more plausible that neutrinos are Majorana fermions and that the scale of lepton violation would be well below the conventional see-saw scale [?] TO DO: *double check this claim*.

Effective neutrino magnetic moment

Since experiments detect neutrino flavour states, not the mass states, what we measure in experiments is an effective "flavour" magnetic moment μ_{eff}. μ_{eff} is influenced by mixing of the neutrino magnetic moments (and electric moments) expressed in the mass basis (as described above) and neutrino oscillations. In the ultra-relativistic limit, the (anti)neutrino effective magnetic moment is

$$\mu^2_{\nu_l}\left(L, E_\nu\right) = \sum_j \left| \sum_k U^{\star}_{lk} e^{\mp i \Delta m^2_{kj} L/2E_\nu} \left(\mu_{jk} - i\epsilon_{jk}\right) \right|^2, \tag{2.13}$$

where L is the distance the neutrino travelled, E_ν is the neutrino energy and δm^2 is the neutrino mass squared difference [?]. The minus sign in the exponent is for neutrinos and the plus sign for antineutrinos, therefore the only difference is in the phase induced by neutrino oscillations.

For experiments with baselines short enough that neutrino oscillations would not have time to develop ($\Delta m^2 L/2E_\nu \ll\sim 1$), such as the NOvA Near Detector, the effective magnetic moment can be expressed as

$$\mu_{\nu_l}^2 = \mu_{\overline{\nu}_l}^2 \simeq \sum_j \left| \sum_k U_{lk}^\star \left(\mu_{jk} - i\epsilon_{jk}\right) \right|^2 = \left[U\left(\mu^2 + \epsilon^2\right)U^\dagger + 2\,\mathrm{Im}\left(U\mu\epsilon U^\dagger\right)\right]_{ll'}, \tag{2.14}$$

which is independent of the neutrino energy and of the source to detector distance.

It is important to mention, that since the effective magnetic moment depends on the flavour of the studied neutrino, it is different (but related) for neutrino experiment studying neutrinos from different sources. Additionally some experiments, namely solar neutrino experiments, need to include matter effects on the neutrino oscillations. Therefore the reports on the value (or upper limit) of the effective neutrino magnetic moment are not directly comparable between different types of neutrino experiments. Theorists publish papers trying to extrapolate the measured effective magnetic moments to each neutrino flavour, but necessarily apply assumptions that might not hold in all BSM theories.

2.1.2 Other neutrino electromagnetic properties

TO DO: *This section is not finished, most of this text is just copied from some theory papers for now*

Neutrino electric charge is heavily constraint by the measurements on the neutrality of matter (since generally neutrinos having an electric charge would also mean that neutrons have charge which would affect all heavier nuclei). It is also constrained by the SN1987A, since neutrino having an effective charge would lengthen its path through the extragalactic magnetic fields and would arrive on earth later. It can also be obtained from nu-on-e scatter from the relationship between neutrino millicharge and magnetic moment. [nuElmagInt2015.pdf - sec. VIIA]

The neutrino charge radius is determined by the second term in the expansion of the neutrino charge form factor and can be interpreted using the Fourier transform of a spherically symmetric charge distribution. It can also be negative since the charge density is not a positively defined quantity. In the SM the charge radius has the form of (possible other definitions exist)

$$\langle r_{\nu_l}^2 \rangle_{\mathsf{SM}} = \frac{G_{\mathsf{F}}}{4\sqrt{2}\pi^2}\left[3 - 2\log\left(\frac{m_l^2}{m_W^2}\right)\right]. \tag{2.15}$$

This corresponds to $\langle r^2_{\nu_\mu} \langle_{\text{SM}} = 2.4 \times 10^{-33}\ \text{cm}^2$ and similar scale for other neutrino flavours. [nuElmagInt2015.pdf - sec. VIIB]

[nuElmagInt2015.pdf - sec. VIIB] The effect of the neutrino charge radius on the neutrino-on-electron scattering cross section is through the following shift of the vector coupling constant (Grau and Grifols, 1986; Degrassi, Sirlin, and VMarciano, 1989; Vogel and Engel, 1989; Hagiwara et al., 1994):

$$g_V^{\nu_l} \to g_V^{\nu_l} + \frac{2}{3} m_W^2 \langle r^2_{\nu_l} \rangle \sin^2\theta_W \tag{2.16}$$

[nuElmagInt2015.pdf - sec. VIIB] The current experimental limits for muon neutrinos are from TO DO: *check the current exp. limits* Hirsch, Nardi, and Restrepo (2003) who obtained the following 90% C.L. bounds on $\langle r^2_{\nu_\mu} \rangle$ from a reanalysis of CHARM-II (Vilain et al., 1995) and CCFR (McFarland et al.,1998) data:

$$-0.52 \times 10^{-32} < \langle r^2_{\nu_\mu} \rangle < 0.68 \times 10^{-32}\ \text{cm}^2 \tag{2.17}$$

In the Standard Model, the neutrino anapole moment is somehow coupled with the neutrino charge radii and is functionally identical. the phenomenology of neutrino anapole moments is similar to that of neutrino charge radii. Hence, the limits on the neutrino charge radii discussed in Sec. VII.B also apply to the neutrino anapole moments multiplied by 6. in the standard model the neutrino charge radius and the anapole moment are not defined separately and one can interpret arbitrarily the charge form factor as a charge radius or as an anapole moment. Therefore, the standard model values for the neutrino charge radii in Eqs. (7.35)–(7.38) can be interpreted also as values of the corresponding neutrino anapole moments. [nuElmagInt2015.pdf - sec. VIIC]

It is possible to consider the toroidal dipole moment as a characteristic of the neutrino which is more convenient and transparent than the anapole moment for the description of T-invariant interactions with nonconservation of the P and C symmetries. the toroidal and anapole moments coincide in the static limit when the masses of the initial and final neutrino states are equal to each other. The toroidal (anapole) interactions of a Majorana as well as a Dirac neutrino are expected to contribute to the total cross section of neutrino elastic scattering off electrons, quarks, and nuclei.

Because of the fact that the toroidal (anapole) interactions contribute to the helicity preserving part of the scattering of neutrinos on electrons, quarks, and nuclei, its contributions to cross sections are similar to those of the neutrino charge radius. In principle, these contributions can be probed and information about toroidal moments can be extracted in low-energy scattering experiments in the future. Different effects of the neutrino toroidal moment are discussed by Ginzburg and Tsytovich (1985), Bukina, Dubovik, and Kuznetsov (1998a, 1998b), and Dubovik and Kuznetsov (1998). In particular, it has been shown that the neutrino toroidal electromagnetic interactions can produce Cherenkov radiation of neutrinos propagating in a medium. [nuElmagInt2015.pdf - sec. VIIC]

2.1.3 Measuring neutrino magnetic moment

The most sensitive method to measure neutrino magnetic moment is the low energy elastic scattering of (anti)neutrinos on electrons [?]. The diagram for this interaction is shown on Fig.2.2 showing the two observables, the recoil electron's kinetic energy ($T_e = E_{e\prime} - m_e$) and the recoil angle with respect to the incoming neutrino beam (θ).

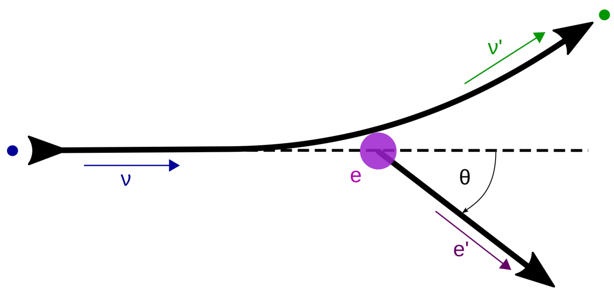

Figure 2.2: Neutrino-on-electron elastic scattering diagram

From simple $2 \to 2$ kinematics we can calculate

$$(P_\nu - P_{e'})^2 = (P_{\nu'} - P_e)^2\,, \tag{2.18}$$

$$m_\nu^2 + m_e^2 - 2E_\nu E_{e'} + 2E_\nu p_{e'} \cos\theta = m_\nu^2 + m_e^2 - 2E_{\nu'} m_e. \tag{2.19}$$

Using the energy conservation

$$E_\nu + m_e = E_{\nu'} + E_{e'} = E_{\nu'} + T_e + m_e \Rightarrow E_{\nu'} = E_\nu - T_e \tag{2.20}$$

we get

$$E_\nu p_{e'}\cos\theta = E_\nu E_{e'} - E_{\nu'} m_e = E_\nu\left(T_e + m_e\right) - \left(E_\nu - T_e\right) m_e = T_e\left(E_\nu + m_e\right), \tag{2.21}$$

$$\cos\theta = \frac{E_\nu + m_e}{E_\nu}\sqrt{\frac{T_e^2}{E_{e'}^2 - m_e^2}} = \frac{E_\nu + m_e}{E_\nu}\sqrt{\frac{T_e^2}{T_e^2 + 2T_e m_e}}. \tag{2.22}$$

And finally we get

$$\cos\theta = \frac{E_\nu + m_e}{E_\nu}\sqrt{\frac{T_e}{T_e + 2m_e}}. \tag{2.23}$$

We can rearrange the Eq. 2.23 to get

$$T_e = \frac{2m_e E_\nu^2\cos^2\theta}{\left(E_\nu + m_e\right)^2 - E_\nu^2\cos^2\theta}. \tag{2.24}$$

Electron's kinetic energy is therefore kinematically constrained by the energy conservation as

$$T_e \leq \frac{2E_\nu^2}{2E_\nu + m_e}, \tag{2.25}$$

which corresponds to the $\cos\theta \to 1$ when the recoil electron goes exactly forward in the incident neutrino direction.

Considering $E_\nu \sim$ GeV, we can approximate $\frac{m_e^2}{E_\nu^2} \to 0$ and from Fig.2.3 we can see that we can approximate all recoil angles to be very small, therefore $\theta^2 \cong (1 - \cos^2\theta)$. Using Eq.2.23 we get

$$T_e\theta^2 \cong T_e\left(1 - \left(\frac{E_\nu + m_e}{E_\nu}\right)^2\frac{T_e}{T_e + 2m_e}\right) = T_e\left(1 - \left(1 + \frac{2m_e}{E_\nu}\right)\frac{T_e}{T_e + 2m_e}\right), \tag{2.26}$$

therefore

$$T_e\theta^2 \cong \frac{2m_e T_e}{T_e + 2m_e}\left(1 - \frac{T_e}{E_\nu}\right) = 2m_e\left(\frac{1}{1 + \frac{2m_e}{T_e}}\right)\left(1 - \frac{T_e}{E_\nu}\right), \tag{2.27}$$

and finally

$$T_e\theta^2 \cong 2m_e\left(1 - \frac{T_e}{E_\nu}\right) < 2m_e. \tag{2.28}$$

This is a strong limit that clearly distinguishes the neutrino-on-electron elastic scattering events from other similar interaction involving single electron (mainly the ν_e Charged Current interaction).

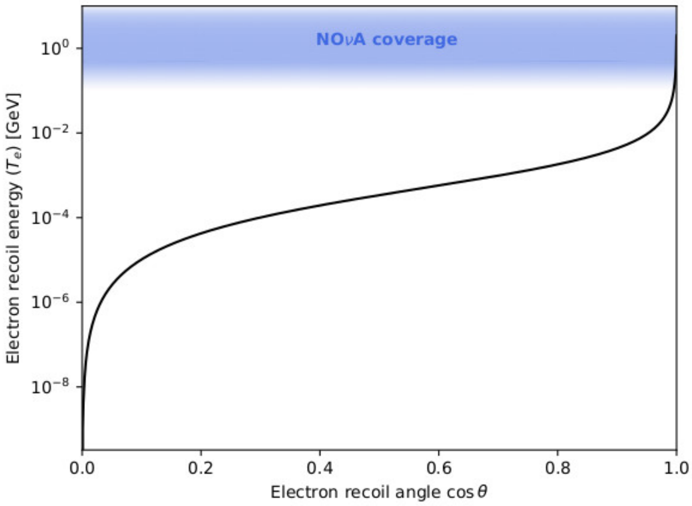

Figure 2.3: Relation between the recoil electron's kinetic energy and angle for neutrino-on-electron elastic scattering. The coverage of the NOvA detectors for measuring the electron recoil energy is shown in blue. Only very forwards electron's are recorded in NOvA.

Neutrino magnetic moment cross section

In the ultrarelativistic limit, the neutrino magnetic moment changes the neutrino helicity, turning active neutrinos into sterile TO DO: *this is a very strong statement and it probably need a bit more backing up*. Since the SM weak interaction conserves helicity we can simply add the two contribution to the neutrino-on-electron cross section incoherently [**?**]:

$$\frac{d\sigma_{\nu_l e^-}}{dT_e} = \left(\frac{d\sigma_{\nu_l e^-}}{dT_e}\right)_{\text{SM}} + \left(\frac{d\sigma_{\nu_l e^-}}{dT_e}\right)_{\text{MAG}} . \tag{2.29}$$

The standard model contribution can be expressed as [**?**]:

$$\left(\frac{d\sigma_{\nu_l e^-}}{dT_e}\right)_{\text{SM}} = \frac{G_F^2 m_e}{2\pi} \left\{ (g_V^{\nu_l} + g_A^{\nu_l})^2 + (g_V^{\nu_l} - g_A^{\nu_l})^2 \left(1 - \frac{T_e}{E_\nu}\right)^2 + \left((g_A^{\nu_l})^2 - (g_V^{\nu_l})^2\right) \frac{m_e T_e}{E_\nu^2} \right\}, \tag{2.30}$$

where the coupling constants g_V and g_A are different for different neutrino flavours ht

Table 2.1: Neutrino-on-electron elastic scattering total cross sections

Process	Total cross section
$\nu_e + e^-$	$\simeq 93 \times 10^{-43} E_\nu \mathrm{cm}^2\mathrm{GeV}^{-1}$
$\overline{\nu}_e + e^-$	$\simeq 39 \times 10^{-43} E_\nu \, \mathrm{cm}^2\mathrm{GeV}^{-1}$
$\nu_{\mu,\tau} + e^-$	$\simeq 15 \times 10^{-43} E_\nu \, \mathrm{cm}^2\mathrm{GeV}^{-1}$
$\overline{\nu}_{\mu,\tau} + e^-$	$\simeq 13 \times 10^{-43} E_\nu \, \mathrm{cm}^2\mathrm{GeV}^{-1}$

and for antineutrinos. Their values are:

$$g_V^{\nu_e} = 2\sin^2\theta_W + 1/2, \qquad g_A^{\nu_e} = 1/2, \tag{2.31}$$

$$g_V^{\nu_{\mu,\tau}} = 2\sin^2\theta_W - 1/2, \qquad g_A^{\nu_{\mu,\tau}} = -1/2. \tag{2.32}$$

For antineutrinos $g_A \to -g_A$.

Using Eq. 2.24 to get the differential cross section on $\cos\theta$:

$$dT_e = \frac{4m_e E_\nu^2 \left(m_e + E_\nu\right)^2}{\left[\left(m_e + E_\nu\right)^2 - E_\nu^2 \cos^2\theta\right]^2} \cos\theta d\cos\theta \tag{2.33}$$

We can also express this as

$$\left(\frac{d\sigma_{\nu_l e^-}}{d\cos\theta}\right)_{\mathsf{SM}} = \frac{2G_F^2 E_\nu^2 m_e^2 \cos\theta \left(E_\nu + m_e\right)^2}{\pi\left(\left(E_\nu + m_e\right)^2 - E_\nu^2\cos^2\theta\right)^2}$$
$$\left\{ (g_V^{\nu_l} + g_A^{\nu_l})^2 + (g_V^{\nu_l} - g_A^{\nu_l})^2 \left(1 - \frac{2m_e E_\nu \cos^2\theta}{\left(E_\nu + m_e\right)^2 - E_\nu^2\cos^2\theta}\right)^2 + \right.$$
$$\left. \left((g_A^{\nu_l})^2 - (g_V^{\nu_l})^2\right) \frac{2m_e^2\cos^2\theta}{\left(\left(E_\nu + m_e\right)^2 - E_\nu^2\cos^2\theta\right)} \right\}, \tag{2.34}$$

[Fundamentals of neutrino Physics and Astrophysics, p.139] The total neutrino-electron elastic scattering cross section for large energies is

The neutrino magnetic moment contribution is TO DO: *include derivation from [?]* [?]:

$$\left(\frac{d\sigma_{\nu_l e^-}}{dT_e}\right)_{\mathsf{MAG}} = \frac{\pi\alpha^2}{m_e^2}\left(\frac{1}{T_e} - \frac{1}{E_\nu}\right)\left(\frac{\mu_{\nu_l}}{\mu_B}\right)^2, \tag{2.35}$$

where α is the fine structure constant.

Comparison of the Standard Model and the neutrino magnetic moment cross sections is shown on Fig.2.4. Whereas the SM cross section is flat with $T_e \to 0$, the νMM cross section keeps increasing to infinity. However, this reach is limited by the experimental capabilities of detecting such low energetic neutrinos. Possible NOvA coverage is shown in a shaded blue and it is uncertain we could actually reach as low as 100 MeV.

TO DO: *Reference the colours on the figures to the origins of the values (LSND and Biao)*

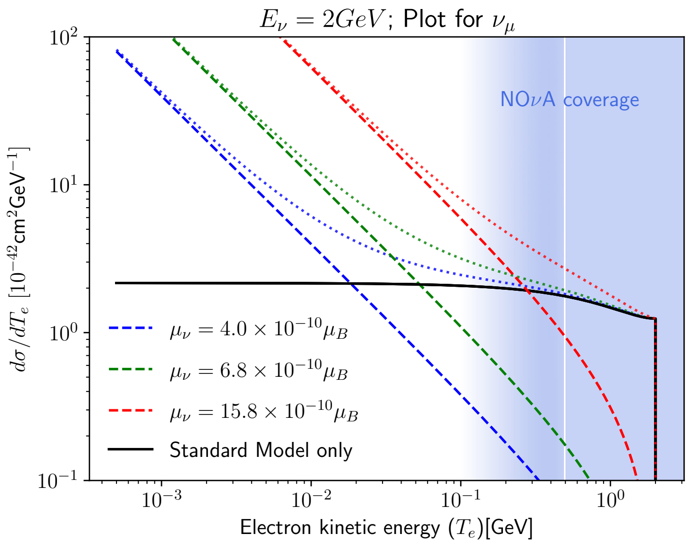

Figure 2.4: Comparison of the neutrino magnetic moment (coloured) and Standard Model (black) cross sections for the neutrino-on-electron elastic scattering. Different colours depict different values of the neutrino magnetic moment. Dashed lines are the individual cross sections and dotted lines are the added total cross section with the standard model contribution. NOvA coverage of electron recoil energies is shown in shaded blue.

As can be seen on Fig.2.4 and Fig.2.5, the magnetic moment contribution exceeds the standard model contribution for low enough T_e. This can be approximated as [?]:

$$T_e \lesssim \frac{\pi^2\alpha^2}{G_F^2 m_e^3}\left(\frac{\mu_\nu}{\mu_B}\right)^2 \simeq 2.9 \times 10^{19}\left(\frac{\mu_\nu}{\mu_B}\right)^2 [\mathrm{MeV}]\,, \tag{2.36}$$

which does not depend on the neutrino energy and makes experiments sensitive to lower energetic electrons more sensitive to the neutrino magnetic moment. This is especially true for the recent dark matter experiments which put stringent limits on the solar neutrino effective magnetic moment, as described in the following section.

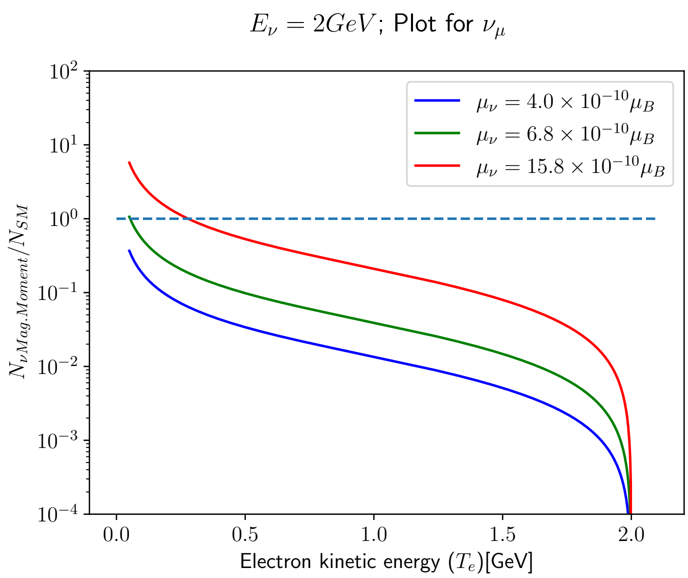

Figure 2.5: Ratio of the netrino magnetic moment cross section to the standard model cross section for the neutrino-on-electron elastic scattering. Different colours depict different effective muon neutrino magnetic moment values.

Acronyms

2p2h two particle - two hole. 7

CC Charged current. 2, 3, 5–7, 10

CEvNS Coherent Elastic ν Nucleus Scattering. 6

COHπ Coherent pion production. 7

CP Charge conjugation - Parity (symmetry). 9

DIS Deep Inelastic Scattering. 6

FSI Final State Interaction. 6, 7

MEC Meson Exchange Current. 6, 7

MSW Mikheyev-Smirnov-Wolfenstein. 10

NC Neutral Current. 2–5, 7, 10

PMNS Pontecorvo-Maki-Nakagawa-Sakata. 8, 9

QE Quasi Elastic (interaction). 5, 7

QED Quantum Electro Dynamics. 5

Res Resonant baryon production. 6

SK Super-Kamiokande. 9

SM Standard Model. 2, 3

SNO Sudbury Neutrino Observatory. 10

Bibliography

[1] Wolfgang Pauli. Pauli letter collection: letter to Lise Meitner. Typed copy. URL http://cds.cern.ch/record/83282.

[2] L. M. Brown. The idea of the neutrino. *Physics Today*, 31(9):23–28, September 1978. doi:10.1063/1.2995181. (Including translation of W. Pauli, Aufsdtze und Vortrdge u'ber Physik und Erkenntnistheorie, Braunschweig (1961)).

[3] H. A. Bethe. Ionization power of a neutrino with magnetic moment. *Mathematical Proceedings of the Cambridge Philosophical Society*, 31(1):108–115, 1935. doi:10.1017/S0305004100012998.

[4] Enrico Fermi. Tentativo di una teoria dei raggi β. 11(1):1–19. ISSN 1827-6121. doi:10.1007/BF02959820.

[5] Fred L. Wilson. Fermi's theory of beta decay. *American Journal of Physics*, 36 (12):1150–1160, 1968. doi:10.1119/1.1974382. (A complete English translation of E.Fermi, Zeitschrift fur Physik 88, 161 (1934)).

[6] Sheldon L. Glashow. Partial-symmetries of weak interactions. 22(4):579–588. ISSN 0029-5582. doi:10.1016/0029-5582(61)90469-2. URL https://www.sciencedirect.com/science/article/pii/0029558261904692.

[7] Steven Weinberg. A model of leptons. *Phys. Rev. Lett.*, 19:1264–1266, Nov 1967. doi:10.1103/PhysRevLett.19.1264. URL https://link.aps.org/doi/10.1103/PhysRevLett.19.1264.

[8] Abdus Salam. *Weak and electromagnetic interactions*, pages 244–254. doi:10.1142/9789812795915_0034. URL https://www.worldscientific.com/doi/abs/10.1142/9789812795915_0034.

[9] L. Landau. On the conservation laws for weak interactions. 3(1):127–131. ISSN 0029-5582. doi:10.1016/0029-5582(57)90061-5. URL https://www.sciencedirect.com/science/article/pii/0029558257900615.

[10] T. D. Lee and C. N. Yang. Parity nonconservation and a two-component theory of the neutrino. *Phys. Rev.*, 105:1671–1675, Mar 1957.

doi:10.1103/PhysRev.105.1671. URL https://link.aps.org/doi/10.1103/PhysRev.105.1671.

[11] Abdus Salam. On parity conservation and neutrino mass. *Nuovo Cim.*, 5:299–301, 1957. doi:10.1007/BF02812841.

[12] Peter W. Higgs. Broken symmetries and the masses of gauge bosons. *Phys. Rev. Lett.*, 13:508–509, Oct 1964. doi:10.1103/PhysRevLett.13.508. URL https://link.aps.org/doi/10.1103/PhysRevLett.13.508.

[13] F. Englert and R. Brout. Broken symmetry and the mass of gauge vector mesons. *Phys. Rev. Lett.*, 13:321–323, Aug 1964. doi:10.1103/PhysRevLett.13.321. URL https://link.aps.org/doi/10.1103/PhysRevLett.13.321.

[14] G. S. Guralnik, C. R. Hagen, and T. W. B. Kibble. Global conservation laws and massless particles. *Phys. Rev. Lett.*, 13:585–587, Nov 1964. doi:10.1103/PhysRevLett.13.585. URL https://link.aps.org/doi/10.1103/PhysRevLett.13.585.

[15] Steven Weinberg. A model of leptons. *Phys. Rev. Lett.*, 19:1264–1266, Nov 1967. doi:10.1103/PhysRevLett.19.1264. URL https://link.aps.org/doi/10.1103/PhysRevLett.19.1264.

[16] Carlo Giunti and Chung W. Kim. *Fundamentals of Neutrino Physics and Astrophysics*. 2007. ISBN 978-0-19-850871-7.

[17] F. Reines and C. L. Cowan. Detection of the free neutrino. *Phys. Rev.*, 92:830–831, Nov 1953. doi:10.1103/PhysRev.92.830. URL https://link.aps.org/doi/10.1103/PhysRev.92.830.

[18] Cowan Jr. C.L., Reines F., Harrison F.B., Kruse H.W., and McGuire A.D. Detection of the free neutrino: A confirmation. *Science*, 124(3212):103–104, July 1956. doi:10.1126/science.124.3212.103.

[19] F. Reines and C.L. Cowan. Neutrino physics. *Physics Today*, 10(8):12–18, 1957. doi:10.1063/1.3060455.

[20] B. Adeva et al. Measurement of Z^0 decays to hadrons and a precise determination of the number of neutrino species. *Phys. Lett. B*, 237:136–146, 1990. doi:10.1016/0370-2693(90)90476-M.

[21] S. Schael et al. Precision electroweak measurements on the Z resonance. *Phys. Rept.*, 427:257–454, 2006. doi:10.1016/j.physrep.2005.12.006.

[22] M. C. Goodman. Resource letter anp-1: Advances in neutrino physics. *American Journal of Physics*, 84:309–319, 2016. doi:10.1119/1.4962228.

[23] M. Schwartz. Feasibility of using high-energy neutrinos to study the weak interactions. *Phys. Rev. Lett.*, 4:306–307, Mar 1960. doi:10.1103/PhysRevLett.4.306. URL https://link.aps.org/doi/10.1103/PhysRevLett.4.306.

[24] K. Kodama et al. Observation of tau neutrino interactions. *Phys. Lett. B*, 504: 218–224, 2001. doi:10.1016/S0370-2693(01)00307-0.

[25] K. Kodama et al. Final tau-neutrino results from the DONuT experiment. *Phys. Rev. D*, 78:052002, 2008. doi:10.1103/PhysRevD.78.052002.

[26] William J Marciano and Zohreh Parsa. Neutrino–electron scattering theory*. 29(11):2629. doi:10.1088/0954-3899/29/11/013. URL https://dx.doi.org/10.1088/0954-3899/29/11/013.

[27] J. A. Formaggio and G. P. Zeller. From ev to eev: Neutrino cross sections across energy scales. *Rev. Mod. Phys.*, 84:1307–1341, Sep 2012. doi:10.1103/RevModPhys.84.1307. URL https://link.aps.org/doi/10.1103/RevModPhys.84.1307.

[28] Jr. Davis, Raymond, Don S. Harmer, and Kenneth C. Hoffman. Search for neutrinos from the sun. *Phys. Rev. Lett.*, 20:1205–1209, 1968. doi:10.1103/PhysRevLett.20.1205.

[29] G. Danby, J-M. Gaillard, K. Goulianos, L. M. Lederman, N. Mistry, M. Schwartz, and J. Steinberger. Observation of high-energy neutrino reactions and the existence of two kinds of neutrinos. *Phys. Rev. Lett.*, 9:36–44, Jul 1962. doi:10.1103/PhysRevLett.9.36. URL https://link.aps.org/doi/10.1103/PhysRevLett.9.36.

[30] C.V. Achar, M.G.K. Menon, V.S. Narasimham, P.V.Ramana Murthy, B.V. Sreekantan, K. Hinotani, S. Miyake, D.R. Creed, J.L. Osborne, J.B.M. Pattison, and A.W. Wolfendale. Detection of muons produced by cosmic ray neutrinos deep underground. 18(2):196–199. ISSN 0031-9163. doi:10.1016/0031-9163(65)90712-2. URL https://www.sciencedirect.com/science/article/pii/0031916365907122.

[31] C. V. Achar et al. Observation of a non-elastic cosmic ray neutrino interaction. *Phys. Lett.*, 19:78–80, 1965. doi:10.1016/0031-9163(65)90969-8.

[32] F. Reines, M. F. Crouch, T. L. Jenkins, W. R. Kropp, H. S. Gurr, G. R. Smith, J. P. F. Sellschop, and B. Meyer. Evidence for high-energy cosmic-ray neutrino interactions. *Phys. Rev. Lett.*, 15:429–433, Aug 1965. doi:10.1103/PhysRevLett.15.429. URL https://link.aps.org/doi/10.1103/PhysRevLett.15.429.

[33] *Fundamental Physics at the Intensity Frontier*, 5 2012. doi:10.2172/1042577.

[34] D. Casper. The Nuance neutrino physics simulation, and the future. *Nucl. Phys. B Proc. Suppl.*, 112:161–170, 2002. doi:10.1016/S0920-5632(02)01756-5.

[35] A. A. Aguilar-Arevalo et al. First measurement of the muon neutrino charged current quasielastic double differential cross section. *Phys. Rev. D*, 81:092005, May 2010. doi:10.1103/PhysRevD.81.092005. URL https://link.aps.org/doi/10.1103/PhysRevD.81.092005.

[36] M. Sajjad Athar, A. Fatima, and S. K. Singh. Neutrinos and their interactions with matter. *Prog. Part. Nucl. Phys.*, 129:104019, 2023. doi:10.1016/j.ppnp.2022.104019.

[37] D. Akimov et al. Observation of coherent elastic neutrino-nucleus scattering. 357(6356):1123–1126. doi:10.1126/science.aao0990. URL https://www.science.org/doi/abs/10.1126/science.aao0990.

[38] M. Martini, M. Ericson, G. Chanfray, and J. Marteau. Unified approach for nucleon knock-out and coherent and incoherent pion production in neutrino interactions with nuclei. *Phys. Rev. C*, 80:065501, Dec 2009. doi:10.1103/PhysRevC.80.065501. URL https://link.aps.org/doi/10.1103/PhysRevC.80.065501.

[39] M. Martini, M. Ericson, G. Chanfray, and J. Marteau. Neutrino and antineutrino quasielastic interactions with nuclei. *Phys. Rev. C*, 81:045502, Apr 2010. doi:10.1103/PhysRevC.81.045502. URL https://link.aps.org/doi/10.1103/PhysRevC.81.045502.

[40] M. Martini, M. Ericson, and G. Chanfray. Neutrino quasielastic interaction and nuclear dynamics. *Phys. Rev. C*, 84:055502, Nov 2011. doi:10.1103/PhysRevC.84.055502. URL https://link.aps.org/doi/10.1103/PhysRevC.84.055502.

[41] B Pontecorvo. Mesonium and antimesonium. *Sov. Phys. JETP*, 33:549–551, 8 1957.

[42] B. Pontecorvo. Inverse beta processes and nonconservation of lepton charge. *Sov. Phys. JETP*, 7:172–173, 1958.

[43] Ziro Maki, Masami Nakagawa, and Shoichi Sakata. Remarks on the unified model of elementary particles. *Prog. Theor. Phys.*, 28:870–880, 1962. doi:10.1143/PTP.28.870.

[44] V. Gribov and B. Pontecorvo. Neutrino astronomy and lepton charge. 28(7): 493–496. ISSN 0370-2693. doi:10.1016/0370-2693(69)90525-5. URL https://www.sciencedirect.com/science/article/pii/0370269369905255.

[45] M.C. Gonzalez-Garcia and Yosef Nir. Neutrino Masses and Mixing: Evidence and Implications. *Rev. Mod. Phys.*, 75:345–402, 2003. doi:10.1103/RevModPhys.75.345.

[46] M. Aglietta et al. Experimental study of atmospheric neutrino flux in the NUSEX experiment. *Europhysics Letters (EPL)*, 8(7):611–614, apr 1989. doi:10.1209/0295-5075/8/7/005. URL https://doi.org/10.1209%2F0295-5075%2F8%2F7%2F005.

[47] K. Daum et al. Determination of the atmospheric neutrino spectra with the fréjus detector. *Zeitschrift für Physik C Particles and Fields*, 66(3):417–428, 1995. ISSN 1431-5858. URL https://doi.org/10.1007/BF01556368.

[48] R. Becker-Szendy et al. Electron- and muon-neutrino content of the atmospheric flux. *Phys. Rev. D*, 46:3720–3724, Nov 1992. doi:10.1103/PhysRevD.46.3720. URL https://link.aps.org/doi/10.1103/PhysRevD.46.3720.

[49] Y. Fukuda et al. Atmospheric muon-neutrino / electron-neutrino ratio in the multiGeV energy range. *Phys. Lett. B*, 335:237–245, 1994. doi:10.1016/0370-2693(94)91420-6.

[50] Y. Fukuda et al. Evidence for oscillation of atmospheric neutrinos. *Phys. Rev. Lett.*, 81:1562–1567, 1998. doi:10.1103/PhysRevLett.81.1562.

[51] Q.R. Ahmad et al. Direct evidence for neutrino flavor transformation from neutral current interactions in the Sudbury Neutrino Observatory. *Phys. Rev. Lett.*, 89:011301, 2002. doi:10.1103/PhysRevLett.89.011301.

[52] L. Wolfenstein. Neutrino oscillations in matter. *Phys. Rev. D*, 17:2369–2374, May 1978. doi:10.1103/PhysRevD.17.2369. URL https://link.aps.org/doi/10.1103/PhysRevD.17.2369.

[53] S.P. Mikheyev and A.Yu. Smirnov. Resonance Amplification of Oscillations in Matter and Spectroscopy of Solar Neutrinos. *Sov. J. Nucl. Phys.*, 42:913–917, 1985.

[54] Patrick Huber et al. Snowmass Neutrino Frontier Report. In *Snowmass 2021*, 11 2022.

[55] Ivan Esteban, M. C. Gonzalez-Garcia, Michele Maltoni, Thomas Schwetz, and Albert Zhou. The fate of hints: updated global analysis of three-flavor neutrino oscillations. *JHEP*, 09:178, 2020. doi:10.1007/JHEP09(2020)178.

[56] Mohammad Sajjad Athar et al. Status and perspectives of neutrino physics. *Prog. Part. Nucl. Phys.*, 124:103947, 2022. doi:10.1016/j.ppnp.2022.103947.